



A comparison of structure, bonding and non-covalent interactions of aryl halide and diarylhalonium halogen-bond donors

Nicole Javaly, Theresa M. McCormick and David R. Stuart*

Full Research Paper

Open Access

Address:

Department of Chemistry, Portland State University, 1719 SW 10th Ave, Portland OR 97201, United States

Email:

David R. Stuart* - dstuart@pdx.edu

* Corresponding author

Keywords:

aryl halide; diarylhalonium; halogen; halogen bond; non-covalent interaction

Beilstein J. Org. Chem. **2024**, *20*, 1428–1435.

<https://doi.org/10.3762/bjoc.20.125>

Received: 26 March 2024

Accepted: 18 June 2024

Published: 27 June 2024

This article is part of the thematic issue "Hypervalent halogen chemistry".

Guest Editor: T. Gulder



© 2024 Javaly et al.; licensee Beilstein-Institut.
License and terms: see end of document.

Abstract

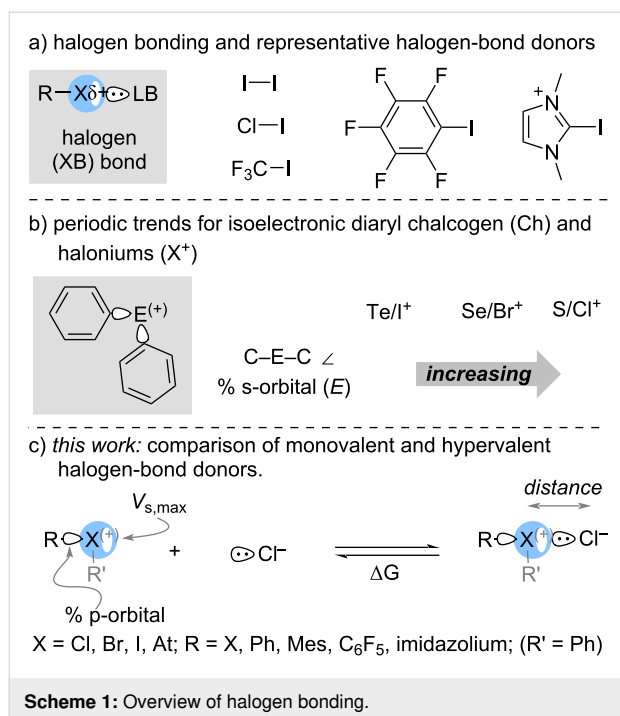
Halogen bonding permeates many areas of chemistry. A wide range of halogen-bond donors including neutral, cationic, monovalent, and hypervalent have been developed and studied. In this work we used density functional theory (DFT), natural bond orbital (NBO) theory, and quantum theory of atoms in molecules (QTAIM) to analyze aryl halogen-bond donors that are neutral, cationic, monovalent and hypervalent and in each series we include the halogens Cl, Br, I, and At. Within this diverse set of halogen-bond donors, we have found trends that relate halogen bond length with the van der Waals radii of the halogen and the non-covalent or partial covalency of the halogen bond. We have also developed a model to calculate ΔG of halogen-bond formation by the linear combination of the % p-orbital character on the halogen and energy of the σ -hole on the halogen-bond donor.

Introduction

Halogen bonding has emerged as an important attractive interaction in a wide range of applications that include crystal engineering, drug discovery and light-emitting materials [1-4]. Although, halogen bonding was first “observed” over 200 years ago [5,6] and the structural characteristics were elucidated in the latter half of the nineteenth century [7], the term “halogen bond” entered the chemical literature in the latter half of twentieth century [8]. Detailed studies of halogen bonding that followed in the late 1990s and early 2000s primarily focused on inorganic molecular and interhalogens, and inorganic and

organic halides that are monovalent (Scheme 1a) [1-4]. Hypervalent halogen compounds, specifically diaryliodonium salts, have also been known to form Lewis acid–base adducts [9,10] and a relative scale to quantify this property has recently been reported [11,12]. Consequently, there has been a recent surge in the use of diarylhalonium salts in halogen-bonding catalysis [13-19].

Crabtree has outlined the similarity in molecular orbitals (MO) formed in halogen bonds and hypervalent bonds (and hydrogen



bonds) [20]. Recently, we [21], and Legault and Huber [22], independently investigated the connection between electronic structure (bonding) and molecular structure (geometry) in diarylhalonium salts. We found a periodic trend with respect to the percentage of *s*- and *p*-orbital character used by the central atom to bond to the aryl substituents for a series of isoelectronic diaryl chalcogen and diarylhalonium compounds (Scheme 1b) [21]. The amount of *s*-character in the orbital used by the central atom (both chalcogen and halogen) to bond with the aryl groups decreases moving down the respective group (16 and 17) [21]. We also found with a limited set of six compounds that the association constant (K_a) for the halogen-bond interaction of diarylhalonium salts with pyridine decreased with increasing *s*-character used by the central halogen atom in the bond opposite the halogen bond; this is effectively the *s*-character in the σ^* -orbital [21].

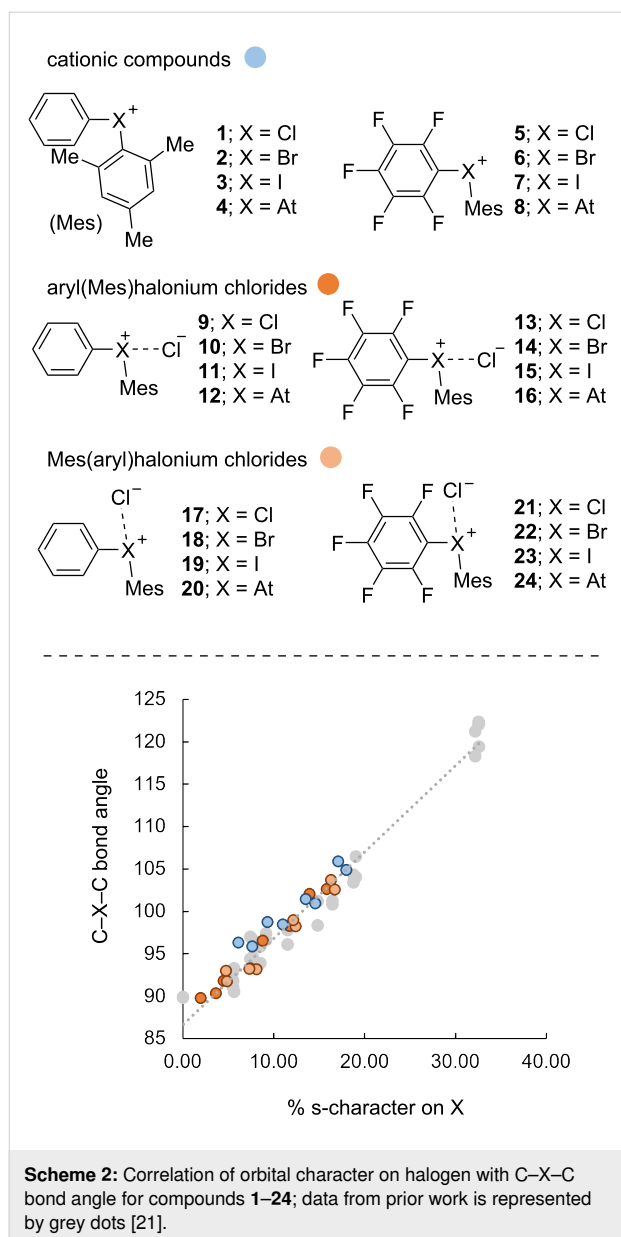
Conceptually, halogen-bond donors are commonly described by the electropositive σ -hole region, which is quantitatively described by $V_{s,max}$ on the halogen, though other factors have also been considered (Scheme 1a) [1-4,23-25]. Huber and co-workers have posed the question: “Is There a Single Ideal Parameter for Halogen-Bonding Based Lewis Acidity?”, and concluded that, for a set of monovalent iodine-based halogen-bond donors, a linear combination of σ -hole and σ^* energy provides a superior predictive ability than σ -hole alone [26]. In this work we compare a set of both monovalent and nominally hypervalent halogen-bond donors in which the central halogen atom is Cl, Br, I, and At. We have used density functional

theory (DFT) to uncover periodic trends in the orbitals used by the central halogen atom in forming covalent and non-covalent interactions and how this impacts the interatomic distance and energy of halogen-bond interactions (Scheme 1c).

Results and Discussion

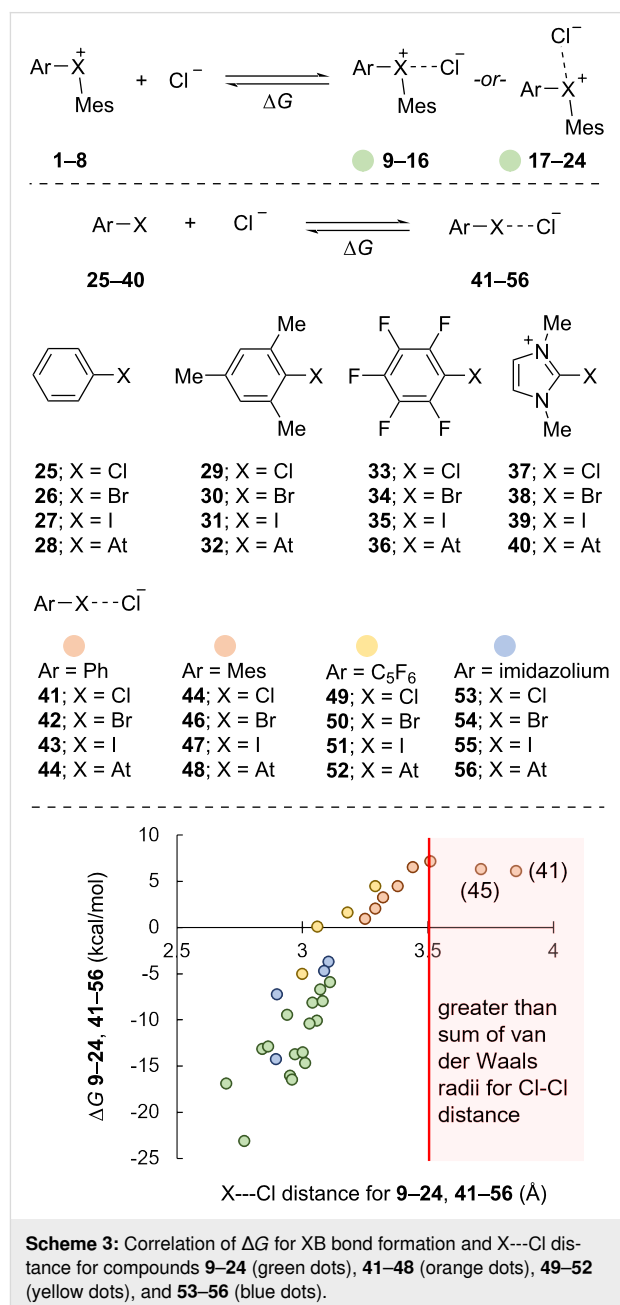
This study evolved from a parallel exploration of reactions involving unsymmetrical phenyl(mesityl)halonium salts, i.e., $\text{Ph}(\text{Mes})X^+$. DFT analysis revealed similar structural trends to our previous work [21] when we expanded the halogens to include astatine (At). Due to its radioactivity and short half-life it would be very challenging to synthesize astatine analogs of diarylhalonium salts and almost no experimental data exists on halogen bonding with astatine for comparison with DFT-generated data. However, the inclusion of molecules containing At in this study provides an opportunity to expand the theoretical framework describing the structure, bonding, and reactivity of diarylhalonium compounds [27]. Although some relativistic effects of astatine may not be sufficiently incorporated in calculations [28], others have shown in theoretical and limited experimental studies that astatine does engage in halogen-bonding interactions [29,30]. In this work, a series of halogen-bond donor molecules and their halogen bond complexes with chloride anion were optimized at the M062x/6-311+G(d) level of theory [31] with def2-tzvpp used for iodine and astatine, and with SMD solvation in tetrahydrofuran (THF) incorporating Huber, Truhlar, and Cramer’s correction for bromine and iodine [32] using Gaussian 09 [33]. Our prior work on the orbital analysis of diarylhalonium salts [21], showed good agreement between crystal structure data and energy-minimized structures at the B3LYP/cc-pvtz level with def2-qzvpp for iodine and tellurium and in the gas phase. In our present work using M06-2x/6-311+G(d) with def2-tzvpp for iodine and astatine, we observed excellent agreement in the correlation between orbitals used on the halonium center and the C–X–C bond angle, i.e., molecular geometry, from our prior work (Scheme 2).

Given the similarities drawn between hypervalent and halogen bonding [20], we considered the association of the diarylhalonium cations **1–8** with chloride anion as well as the association of the monovalent subunits **25–36** with chloride anion (Scheme 3). We also considered the association of cationic monovalent halogen-bond donors **37–40** with chloride as the imidazolium iodide is a well-established core of halogen-bonding catalysts [34,35] (Scheme 3). In general, we observed that more exergonic association of the halogen-bond donors with chloride were associated with closer X---Cl contacts (Scheme 3). The monovalent halogen-bond donors of phenyl, mesityl, and pentafluorophenyl derivatives **25–35** had endergonic association with chloride (Scheme 3). Pentafluorophenyl astatide (**36**) was the only neutral monovalent halogen-bond

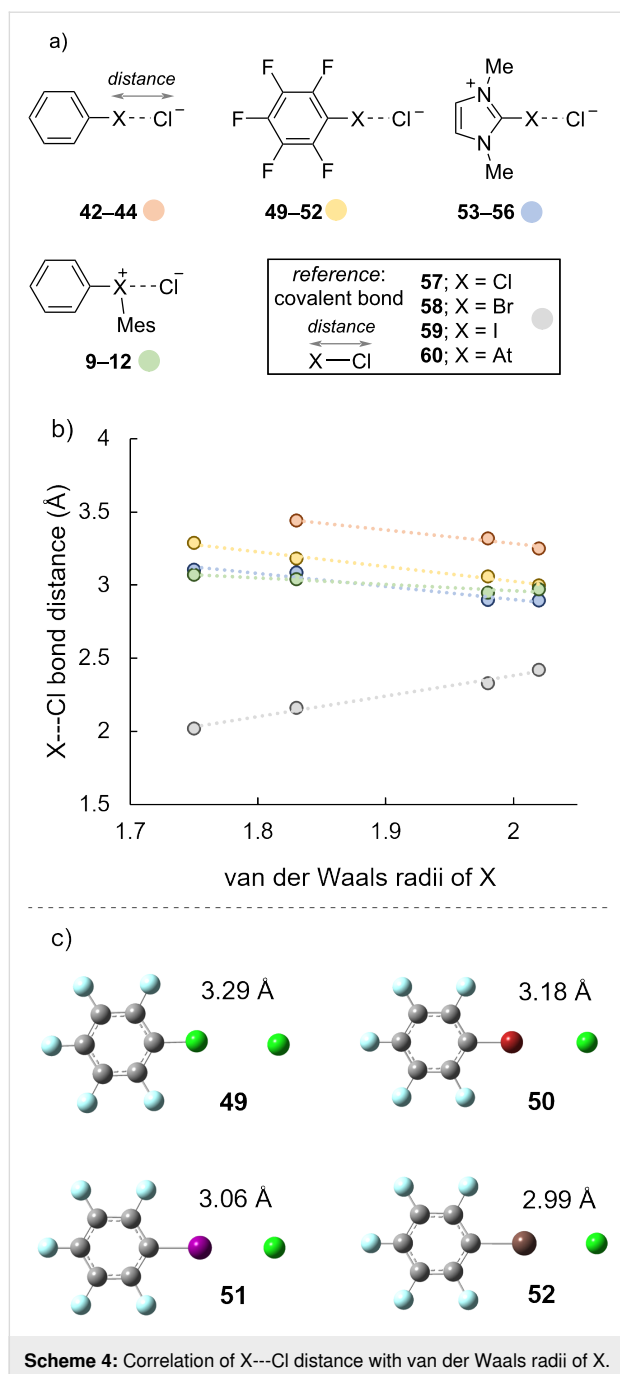


donor with an exergonic association with chloride ($\Delta G = -5.0$ kcal/mol). The X---Cl distance calculated for the halogen-bonding complexes **41** and **45** of phenyl chloride (**25**) and mesityl chloride (**29**) with chloride anion were 3.85 and 3.71 Å, respectively. These values are larger than the sum of the van der Waals radii (3.5 Å) for two chlorine atoms [36] and therefore unlikely to represent a substantial halogen-bonding interaction. The hypervalent halogen-bond donors **1–8** had substantially more exergonic association with chloride than their monovalent subunits. For instance, the association of chloride with pentafluorophenyl bromide (**34**) was $\Delta G = 1.6$ kcal/mol, whereas the association of chloride with pentafluorophenyl(mesityl)bromonium (**6**) was $\Delta G = -13.2$ kcal/mol. The overall charge on the halogen-bond donor also has an impact on

the energy of association. The association of chloride with the diarylhalonium cations **1–8** had ΔG values that ranged from -5.9 to -23.1 kcal/mol (see Supporting Information File 1 for exact values). Likewise, the association of chloride with imidazolium halides **37–40** ranged from -3.7 to -14.3 kcal/mol, which overlaps with the range observed for the diarylhalonium cations.



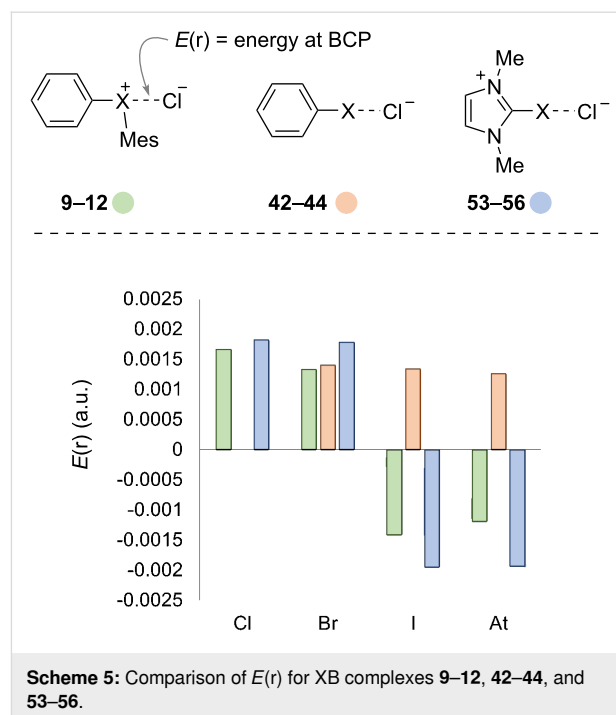
We delved deeper into the periodic trends related to the X---Cl distance for halogen-bond complexes **9–24**, **42–44**, and **46–56**; representative examples are shown in Scheme 4. As a reference we considered the trend in X-Cl covalent bond distance with



respect to the van der Waals radii of X [36], and we observed a linear trend with a positive slope (Scheme 4b, grey dots). That is the length of the X—Cl (57–60) covalent bond increases with increasing van der Waals radii of X. Notably, this trend is also replicated for ionic bonds of the halides with sodium; longer ionic bond lengths are observed for larger halides [37]. On the other hand, halogen-bond complexes that we studied here revealed an opposite trend (Scheme 4b, orange, yellow, blue, and green dots). The halogen-bond length decreased with increasing van der Waals radii of X and the trend was more pro-

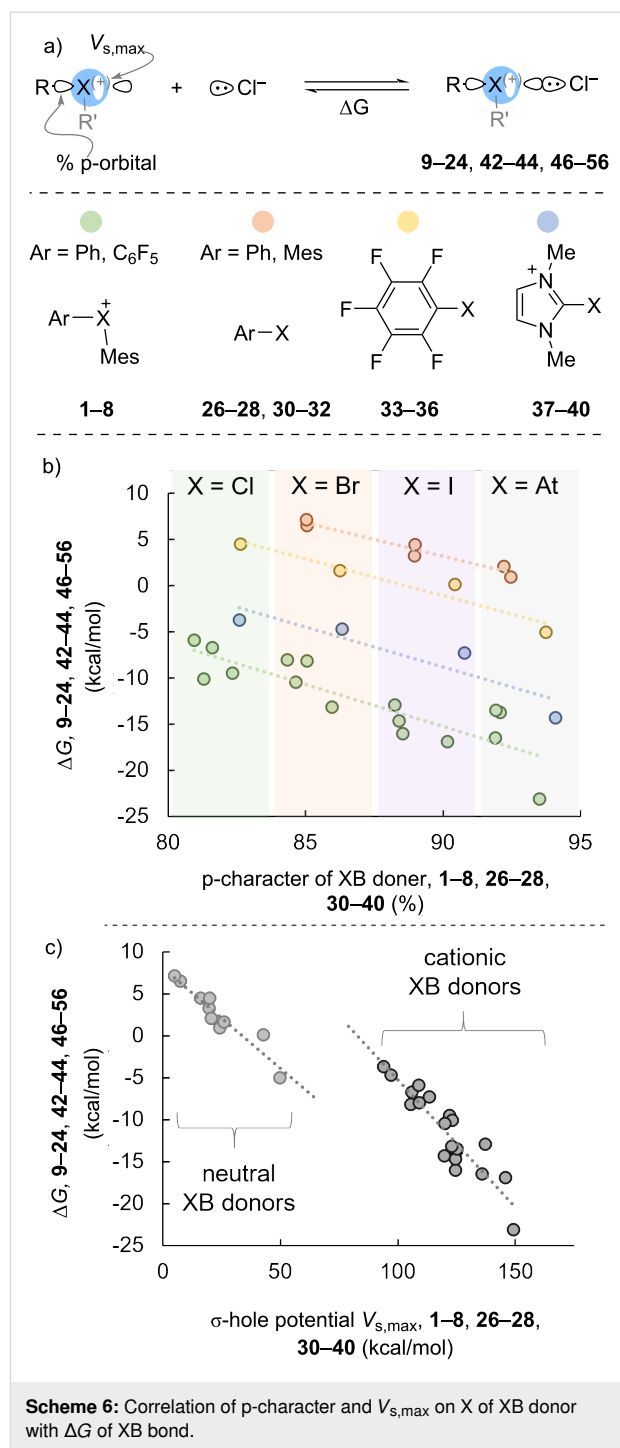
nounced for monovalent halogen-bond donors. This is exemplified by halogen-bond complexes of the pentafluorophenyl halide series with chloride anion (Scheme 4c, 49–52). A similar trend for decreasing bond length with increasing van der Waals radii has also been observed for some [38], though not all [39], series of chalcogen bonds. Generally, shorter bonds are stronger and longer bonds are weaker, and the trend we observe here for halogen bonding aligns with that rule of thumb (Scheme 3). The conceptual frameworks underpinning covalent and ionic bonds are orbital overlap and electrostatic attraction, respectively. Therefore, if larger van der Waals radii are associated with longer, weaker bonds where both these phenomena (orbital overlap and electrostatics) are operative (covalent and ionic bonds), our observations suggest a unique feature of halogen bonding that relates to bond length. Pauli repulsion and dispersion are additional factors that have been included in defining halogen bonds [25]. Smaller halogens that are less able to disperse lone-pairs may have greater destabilizing repulsive forces associated with them that ultimately lengthen the halogen bond relative to those of larger halogens [22,40].

Further analysis of the XB complexes revealed additional distinctions in the nature of the halogen bonds (Scheme 5). We used Bader's quantum theory of atoms in molecules (QTAIM) [41] and assessed $\rho(r)$, $\nabla^2(r)$, and associated values. However, to minimize complexity we elected to focus on the distance between the bond critical points (BCP) and the atomic centers (available in Supporting Information File 1, Table S8) and the electronic energy at the BCPs, $E(r)$ (Scheme 5). On the bond-



ing continuum positive values of $E(r)$ are generally associated non-covalent bonds and negative values of $E(r)$ indicate increasing covalency [42]. We observed a switch from positive $E(r)$ values for the lighter hypervalent phenyl(mesityl)haloniums **9** and **10** ($X = \text{Cl}$ and Br) to negative $E(r)$ values for the heavier haloniums **11** and **12** ($X = \text{I}$ and At , Scheme 5, green bars). Uchiyama previously suggested that the diarylchloronium **9** has a “breakdown of the hypervalent bond” [43], and our data suggest that the interaction (halogen or hypervalent bond) between chloride anion and diarylchloronium cation **9** is non-covalent and likely dominated by electrostatic attraction. A similar switch from non-covalent halogen bond for the lighter ($X = \text{Cl}$ and Br) to partially covalent halogen bond for the heavier ($X = \text{I}$ and At) was also observed for the cationic imidazolium series of XB donors **53–56** (Scheme 5, blue bars). The neutral monovalent XB donors **26–28** formed halogen-bonding complexes **42–44** with non-covalent interactions in all cases, even those with heavier halogen iodine and astatine (Scheme 5, orange bars).

We turned our attention from periodic trends in XB length to periodic trends in XB strength. The σ -bond oriented 180° relative to the halogen bond plays a central role in tuning the halogen bond properties [1–4]. Indeed, it impacts the size of the σ -hole ($V_{s,\text{max}}$), and the energy of the σ^* orbital has been shown to be a key component of a predictive model for halogen-bond strength [26]. However, a confounding, though rarely discussed, factor for halogen-bond strength is the composition (s/p-character) of the orbital on the halogen atom that is engaged in the σ -bond (Scheme 6a). We have previously shown that larger association constants (K_{eq}) were measured for hypervalent halogen-bond donors with greater calculated p-character on the halogen participating in the σ -bond opposite the hypervalent (or halogen) bond; both K_{eq} and p-character on X increased in the order $\text{Cl} < \text{Br} < \text{I}$ [21]. We conducted a similar analysis here in which we plotted the percent p-orbital contribution on the XB donor against ΔG determined by DFT (Scheme 6b). Although, we found that this feature is a poor global predictor of ΔG , clear periodic trends are observed when related groups of XB donors are considered (Scheme 6b). When the halogen-bond donors are clustered into hypervalent **1–8** (Scheme 6b, green dots), monovalent aryl **26–28** and **30–32** (Scheme 6b, orange dots), perfluorophenyl **33–36** (Scheme 6b, yellow dots), and imidazolium **37–40** (Scheme 6b, blue dots) linear correlations with similar slopes are observed for p-orbital character and ΔG (Scheme 6b). Analysis in this way also provides an opportunity for comparison between these groups for the same halogen, that is a comparison between monovalent and hypervalent halogen-bond donors, and neutral and cationic halogen-bond donors. First, when the halogen is held constant it can be seen that the different classes of halogen-bond donors (monovalent vs hyperva-



lent) use similar orbital composition to form the σ -bond with the aryl group (Scheme 6b). The percentage of p-character in the σ -orbital for halogen-bond donors with $X = \text{Cl}$ is ≈ 80 – 82% , $X = \text{Br}$ is ≈ 84 – 86% , $X = \text{I}$ is ≈ 88 – 91% , and $X = \text{At}$ is ≈ 92 – 94% . Interestingly, monovalent halogen-bond donors use slightly more p-orbital character to bond with the aryl group than their hypervalent counterparts. For example, in phenyl iodide (**27**) the iodine atom uses 88.97% p-character to bond with the phe-

nyl group, whereas in phenyl(mesityl)iodonium cation (**3**) the iodine atom uses 88.54% p-character to bond with the phenyl group. Phenyl iodide (**27**) has three lone-pairs, whereas the phenyl(mesityl)iodonium cation (**3**) has two lone-pairs (though it does have another aryl group), and therefore this observation is consistent with Bent's rule in which lone-pairs are stabilized by being in orbitals with more s-character [44]. An additional observation regarding the p-character directed at the aryl group by the halogen center relates to the charge on the halogen-bond donor. The halogen of the cationic imidazolium halogen-bond donors **37–40** has the largest amount of p-orbital character in bonding with the aryl group, this was followed by the perfluorophenyl monovalent halogen bond donors **33–36**, then monovalent aryl halogen-bond donors **26–28** and **30–32**, and finally hypervalent halogen-bond donors **1–8**. This observation is also consistent with Bent's rule in which greater p-character is directed toward more electronegative ligands [44].

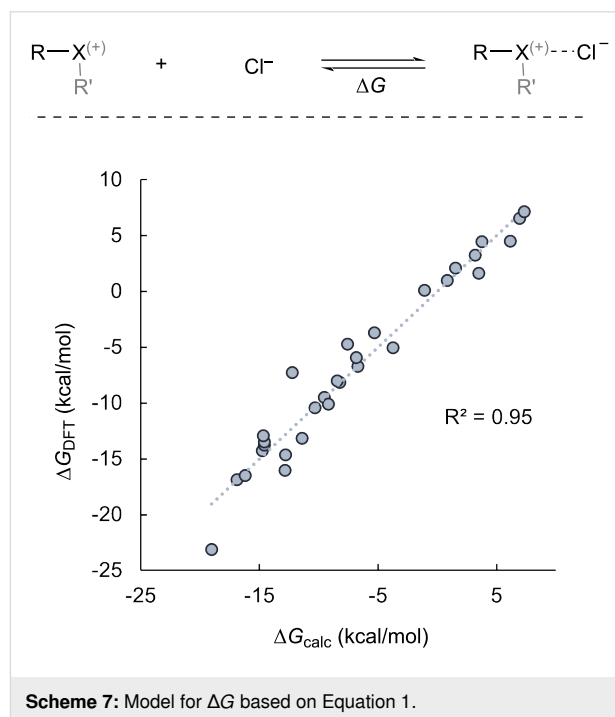
We also consider a correlation between $V_{s,max}$ of the halogen-bond donor and ΔG of the halogen bond (Scheme 6c) [45]. Although a modest linear correlation ($R^2 = 0.90$) was observed over all data points, in which XB donors with larger $V_{s,max}$ values also had more exergonic associations, we actually observed two almost parallel clusters of data (Scheme 6c). In this case, neutral XB donors **26–28**, and **30–36** had $V_{s,max}$ values ≈ 5 – 50 kcal/mol and a slope of -0.24 (Scheme 6c, light grey dots), whereas cationic XB donors **1–8** and **37–40** had $V_{s,max}$ values ≈ 100 – 150 kcal/mol and a slope of -0.30 (Scheme 6c, dark grey dots). So, the distinction in our data set regarding $V_{s,max}$ is not between monovalent and hypervalent halogen-bond donors, but rather between neutral and cationic halogen-bond donors. Three additional points regarding these data sets warrant comment. First, within the neutral XB donors it is perhaps not surprising that perfluoroaryl XB donors **32–36** had substantially larger $V_{s,max}$ values than their non-fluorinated counter parts. Second, two data points are especially representative of the discontinuity in these data sets, the pentafluorophenyl astatide XB donor **36** has a $V_{s,max} = 49.8$ kcal/mol and $\Delta G = -5.0$ kcal/mol, on the other hand cationic imidazolium chloride XB donor **37** has a $V_{s,max} = 94.0$ kcal/mol (almost two fold that of **36**) yet has a $\Delta G = -3.7$ kcal/mol (less than that of **36**). Third, within the cationic XB donors the hypervalent haloniums **1–8** in which the positive charge is primarily located on the halogen had larger $V_{s,max}$ values than the imidazolium halides **37–40** in which the positive charge is primarily delocalized on the imidazolium ring.

We have developed a model for ΔG of the halogen bonds investigated in this work by merging the two concepts of p-orbital character and $V_{s,max}$ of the XB donor (Scheme 7). Although we considered other characteristics of XB donors, including NPA

charges and Hirshfeld charges (available in Supporting Information File 1, Table S5), the linear combination of p-character (%) and σ -hole ($V_{s,max}$) provided the highest correlation based on linear regression analysis of ΔG_{DFT} vs ΔG_{calc} , wherein ΔG_{calc} is obtained from Equation 1 [46].

$$\Delta G_{calc} = -1.95 (\% \text{ p orbital}) - 7.56 (V_{s,max}) - 6.78 \quad (1)$$

Our model was developed with normalized parameters of % p-orbital character and $V_{s,max}$ and therefore a comparison of the parameter coefficients reveals that $V_{s,max}$ is a more dominant term than % p-orbital character in predicting ΔG (Equation 1 and Scheme 7). However, the % p-character term is non-negligible and demonstrates that this highly intuitive parameter contributes to the prediction of ΔG for halogen bonding. It is important to point out that this model is limited to the halogen-bond donors studied here and their interaction with chloride anion, although it is likely that prediction of ΔG with Equation 1 for structurally similar halogen-bond donors would be successful provided the parameters (% p-character and $V_{s,max}$) are known. However, ΔG cannot be predicted for halogen-bond acceptors other than chloride and a more general predictive model should include parameters to describe the Lewis basic halogen-bond acceptor.



Conclusion

In this work, we have compared the characteristics of monovalent, hypervalent, neutral, and cationic XB donors and their XB

complexes with chloride anion by DFT. The structural characteristics of the diaryliodonium cations (XB donors) and diaryliodonium chloride salts (XB complexes) are consistent with our previous model that correlates s/p-orbital composition and C–X–C bond angle. The XB complexes that we studied generally follow the heuristic that stronger bonds are associated with shorter bonds. We found, however, that unlike covalent and ionic bonds, the halogen bonds studied decrease in length with increasing van der Waals radii of the halogen, and we suggest that this is possibly due to greater dispersive and lesser repulsive forces for larger halogens. This finding may prove useful in catalyst design where close spatial proximity of the substrate to other important structural information (i.e., chirality) has an impact on selectivity. Our analysis of selected XB complexes by QTAIM revealed that for cationic XB donors of the lighter halogens (X = Cl and Br) have non-covalent halogen bonds and those of the heavier halogens (X = I and At) have partially covalent halogen bonds. Clustered analysis of the XB donor parameters % p-orbital character and σ -hole potential ($V_{s,max}$) showed linear correlations with ΔG_{DFT} of the halogen bond. The linear combination of the normalized parameters (% p-orbital character and $V_{s,max}$) provides a model to calculate ΔG of the halogen bond.

Supporting Information

Supporting Information File 1

Computational data.

[<https://www.beilstein-journals.org/bjoc/content/supplementary/1860-5397-20-125-S1.pdf>]

Supporting Information File 2

Coordinates of optimized structures.

[<https://www.beilstein-journals.org/bjoc/content/supplementary/1860-5397-20-125-S2.xyz>]

Funding

This work was funded by the National Science Foundation (CHE 2154500). The NSF provided funding for the high-performance computing cluster at PSU (DMS 1624776).

Author Contributions

Nicole Javalý: data curation; formal analysis; methodology; visualization; writing – original draft; writing – review & editing. Theresa M. McCormick: conceptualization; formal analysis; funding acquisition; supervision; writing – review & editing. David R. Stuart: conceptualization; formal analysis; funding acquisition; methodology; supervision; visualization; writing – original draft; writing – review & editing.

ORCID® iDs

David R. Stuart - <https://orcid.org/0000-0003-3519-9067>

Data Availability Statement

All data that supports the findings of this study is available in the published article and/or the supporting information to this article.

References

- Cavallo, G.; Metrangolo, P.; Milani, R.; Pilati, T.; Priimagi, A.; Resnati, G.; Terraneo, G. *Chem. Rev.* **2016**, *116*, 2478–2601. doi:10.1021/acs.chemrev.5b00484
- Beale, T. M.; Chudzinski, M. G.; Sarwar, M. G.; Taylor, M. S. *Chem. Soc. Rev.* **2013**, *42*, 1667–1680. doi:10.1039/c2cs35213c
- Gilday, L. C.; Robinson, S. W.; Barendt, T. A.; Langton, M. J.; Mullaney, B. R.; Beer, P. D. *Chem. Rev.* **2015**, *115*, 7118–7195. doi:10.1021/cr500674c
- Kolář, M. H.; Hobza, P. *Chem. Rev.* **2016**, *116*, 5155–5187. doi:10.1021/acs.chemrev.5b00560
- Colin, M. M.; Gaultier de Claubry, H. *Ann. Chim. (Cachan, Fr.)* **1814**, *90*, 87–100.
- Colin, M. M. *Ann. Chim. (Cachan, Fr.)* **1814**, *91*, 252–272.
- Guthrie, F. J. *Chem. Soc.* **1863**, *16*, 239–244. doi:10.1039/j58631600239
- Zingaro, R. A.; Hedges, R. M. *J. Phys. Chem.* **1961**, *65*, 1132–1138. doi:10.1021/j100825a010
- Ochiai, M.; Suefuji, T.; Miyamoto, K.; Tada, N.; Goto, S.; Shiro, M.; Sakamoto, S.; Yamaguchi, K. *J. Am. Chem. Soc.* **2003**, *125*, 769–773. doi:10.1021/ja0211205
- Ochiai, M.; Suefuji, T.; Shiro, M.; Yamaguchi, K. *Heterocycles* **2006**, *67*, 391. doi:10.3987/com-05-s(t)8
- Labattut, A.; Tremblay, P.-L.; Moutounet, O.; Legault, C. Y. *J. Org. Chem.* **2017**, *82*, 11891–11896. doi:10.1021/acs.joc.7b01616
- Mayer, R. J.; Ofial, A. R.; Mayr, H.; Legault, C. Y. *J. Am. Chem. Soc.* **2020**, *142*, 5221–5233. doi:10.1021/jacs.9b12998
- Zhang, Y.; Han, J.; Liu, Z.-J. *RSC Adv.* **2015**, *5*, 25485–25488. doi:10.1039/c5ra00209e
- Heinen, F.; Engelage, E.; Dreger, A.; Weiss, R.; Huber, S. M. *Angew. Chem., Int. Ed.* **2018**, *57*, 3830–3833. doi:10.1002/anie.201713012
- Heinen, F.; Engelage, E.; Cramer, C. J.; Huber, S. M. *J. Am. Chem. Soc.* **2020**, *142*, 8633–8640. doi:10.1021/jacs.9b13309
- Heinen, F.; Reinhard, D. L.; Engelage, E.; Huber, S. M. *Angew. Chem., Int. Ed.* **2021**, *60*, 5069–5073. doi:10.1002/anie.202013172
- Nishida, Y.; Suzuki, T.; Takagi, Y.; Amma, E.; Tajima, R.; Kuwano, S.; Arai, T. *ChemPlusChem* **2021**, *86*, 741–744. doi:10.1002/cplu.202100089
- Yoshida, Y.; Ishikawa, S.; Mino, T.; Sakamoto, M. *Chem. Commun.* **2021**, *57*, 2519–2522. doi:10.1039/d0cc07733j
- Yunusova, S. N.; Novikov, A. S.; Soldatova, N. S.; Vovk, M. A.; Bolotin, D. S. *RSC Adv.* **2021**, *11*, 4574–4583. doi:10.1039/d0ra09640g
- Crabtree, R. H. *Chem. Soc. Rev.* **2017**, *46*, 1720–1729. doi:10.1039/c6cs00688d
- Karandikar, S. S.; Bhattacharjee, A.; Metze, B. E.; Javalý, N.; Valente, E. J.; McCormick, T. M.; Stuart, D. R. *Chem. Sci.* **2022**, *13*, 6532–6540. doi:10.1039/d2sc02332f
- Robidas, R.; Reinhard, D. L.; Huber, S. M.; Legault, C. Y. *ChemPhysChem* **2023**, *24*, e202200634. doi:10.1002/cphc.202200634

23. Řezáč, J.; de la Lande, A. *Phys. Chem. Chem. Phys.* **2017**, *19*, 791–803. doi:10.1039/c6cp07475h
24. Riley, K. E.; Hobza, P. *Phys. Chem. Chem. Phys.* **2013**, *15*, 17742. doi:10.1039/c3cp52768a
25. Thirman, J.; Engelage, E.; Huber, S. M.; Head-Gordon, M. *Phys. Chem. Chem. Phys.* **2018**, *20*, 905–915. doi:10.1039/c7cp06959f
26. Engelage, E.; Reinhard, D.; Huber, S. M. *Chem. – Eur. J.* **2020**, *26*, 3843–3861. doi:10.1002/chem.201905273
27. Rossi, E.; De Santis, M.; Sorbelli, D.; Storchi, L.; Belpassi, L.; Belanzoni, P. *Phys. Chem. Chem. Phys.* **2020**, *22*, 1897–1910. doi:10.1039/c9cp06293a
28. Gamboni, G.; Belpassi, L.; Belanzoni, P. *ChemPhysChem* **2024**, e202400310. doi:10.1002/cphc.202400310
29. Devore, D. P.; Ellington, T. L.; Shuford, K. L. *J. Phys. Chem. A* **2024**, *128*, 1477–1490. doi:10.1021/acs.jpca.3c06894
30. Guo, N.; Maurice, R.; Teze, D.; Graton, J.; Champion, J.; Montavon, G.; Galland, N. *Nat. Chem.* **2018**, *10*, 428–434. doi:10.1038/s41557-018-0011-1
31. Wang, Y.; Verma, P.; Jin, X.; Truhlar, D. G.; He, X. *Proc. Natl. Acad. Sci. U. S. A.* **2018**, *115*, 10257–10262. doi:10.1073/pnas.1810421115
32. Engelage, E.; Schulz, N.; Heinen, F.; Huber, S. M.; Truhlar, D. G.; Cramer, C. J. *Chem. – Eur. J.* **2018**, *24*, 15983–15987. doi:10.1002/chem.201803652
33. *Gaussian 09*, Revision D.01; Gaussian, Inc.: Wallingford, CT, 2013.
34. Gliese, J.-P.; Jungbauer, S. H.; Huber, S. M. *Chem. Commun.* **2017**, *53*, 12052–12055. doi:10.1039/c7cc07175b
35. Sutar, R. L.; Erochok, N.; Huber, S. M. *Org. Biomol. Chem.* **2021**, *19*, 770–774. doi:10.1039/d0ob02503h
36. Mantina, M.; Chamberlin, A. C.; Valero, R.; Cramer, C. J.; Truhlar, D. G. *J. Phys. Chem. A* **2009**, *113*, 5806–5812. doi:10.1021/jp8111556
37. CCCBDB bond length model; NIST Computational Chemistry Comparison and Benchmark Database; NIST Standard Reference Database Number 101, Release 22; May 2022; Russell, D. Johnson, III. <https://cccbdb.nist.gov/bondlengthmodel2x.asp?method=51&basis=20> (accessed March 19, 2024).
38. Oliveira, V.; Cremer, D.; Kraka, E. *J. Phys. Chem. A* **2017**, *121*, 6845–6862. doi:10.1021/acs.jpca.7b06479
39. de Azevedo Santos, L.; van der Lubbe, S. C. C.; Hamlin, T. A.; Ramalho, T. C.; Matthias Bickelhaupt, F. *ChemistryOpen* **2021**, *10*, 391–401. doi:10.1002/open.202000323
40. Ramasami, P.; Murray, J. S. *J. Mol. Model.* **2024**, *30*, 81. doi:10.1007/s00894-024-05869-5
41. Bader, R. F. W. *Chem. Rev.* **1991**, *91*, 893–928. doi:10.1021/cr00005a013
42. Miller, D. K.; Chernyshov, I. Y.; Torubaev, Y. V.; Rosokha, S. V. *Phys. Chem. Chem. Phys.* **2022**, *24*, 8251–8259. doi:10.1039/d1cp05441d
43. Nakajima, M.; Miyamoto, K.; Hirano, K.; Uchiyama, M. *J. Am. Chem. Soc.* **2019**, *141*, 6499–6503. doi:10.1021/jacs.9b02436
44. Bent, H. A. *Chem. Rev.* **1961**, *61*, 275–311. doi:10.1021/cr60211a005
45. Donald, K. J.; Pham, N.; Ravichandran, P. *J. Phys. Chem. A* **2023**, *127*, 10147–10158. doi:10.1021/acs.jpca.3c05797
46. Santiago, C. B.; Guo, J.-Y.; Sigman, M. S. *Chem. Sci.* **2018**, *9*, 2398–2412. doi:10.1039/c7sc04679k

License and Terms

This is an open access article licensed under the terms of the Beilstein-Institut Open Access License Agreement (<https://www.beilstein-journals.org/bjoc/terms>), which is identical to the Creative Commons Attribution 4.0 International License (<https://creativecommons.org/licenses/by/4.0>). The reuse of material under this license requires that the author(s), source and license are credited. Third-party material in this article could be subject to other licenses (typically indicated in the credit line), and in this case, users are required to obtain permission from the license holder to reuse the material.

The definitive version of this article is the electronic one which can be found at:

<https://doi.org/10.3762/bjoc.20.125>